Engineering Science & Technology
https://ojs.wiserpub.com/index.php/EST/

Research Article

A Novel Orthogonal Collocation Approach for Variable-Order Fractional Algebraic-Differential Equations with Applications to RLC Circuits

William Júnio de Lima[1], **Fran Sérgio Lobato**[2*]

[1] Federal Institute of Northern Minas Gerais, Pirapora Campus, Pirapora, MG, Brazil
[2] Faculty of Chemical Engineering, Federal University of Uberlândia, Uberlândia, MG, Brazil
E-mail: fslobato@ufu.br

Received: 13 February 2026; **Revised:** 15 October 2026; **Accepted:** 22 October 2026

Abstract: This work presents a novel extension of the Orthogonal Collocation Method (OCM) for the numerical solution of variable-order fractional differential–algebraic equations with prescribed initial conditions. Unlike most existing collocation-based approaches, the proposed formulation is specifically designed for differential–algebraic systems and accommodates time-dependent fractional orders within the Caputo framework. The methodology is validated using two benchmark mathematical problems and subsequently applied to the analysis of a fractional-order Resistor-Inductor-Capacitor (RLC) electrical circuit under free and forced excitation. The numerical results show excellent agreement with analytical solutions and significant improvements over reference solutions reported in the literature. For the benchmark problems, the proposed approach achieved errors several orders of magnitude smaller than those reported in previous studies and substantially lower than those obtained with the Adams-type Predictor–Corrector Method (APCM). In addition, the method required markedly lower computational times while using only a small number of collocation points. For the RLC circuit, the results indicate that the variable fractional order has a pronounced influence on the system dynamics, often comparable to or greater than that of the electrical resistance. Fractional orders close to unity reproduce the classical circuit behavior, whereas lower orders introduce stronger memory effects, leading to reduced current amplitudes, lower energy dissipation, and enhanced energy storage in the reactive components. The proposed framework provides an accurate and computationally efficient tool for simulating variable-order fractional differential–algebraic systems and offers a promising alternative for modeling complex engineering processes characterized by memory and hereditary effects.

Keywords: Orthogonal Collocation Method (OCM), variable-order fractional derivative, differential–algebraic equations, Resistor-Inductor-Capacitor (RLC) circuit, fractional dynamics, memory effects

1. Introduction

Fractional calculus generalizes classical calculus by allowing integrals and derivatives of non-integer order. Over the past decades, increasing attention has been devoted to fractional models, including variable-order formulations [1], as they provide a flexible framework for describing complex physical phenomena characterized by memory effects, nonlocality, and fractal-like behavior [2]. Depending on the underlying assumptions, fractional differential models may be formulated with constant or variable (dynamic) orders [3]. A key feature of such operators is their intrinsic nonlocality, which enables the natural incorporation of memory and hereditary effects that are characteristic of many real-world processes [4].

Copyright ©2026 Fran Sérgio Lobato, et al.
DOI: https://doi.org/10.37256/est.8120279790
This is an open-access article distributed under a CC BY license
(Creative Commons Attribution 4.0 International License)
https://creativecommons.org/licenses/by/4.0/

In the context of variable-order fractional derivatives, the pioneering contribution of Samko and Ross [5] introduced the concept of fractional differentiation with an order that varies with the independent variable. Soon et al. [6] subsequently demonstrated that allowing the fractional order to vary can enhance the descriptive capability of fractional models by providing additional flexibility to represent the evolving dynamics of physical systems. Since then, variable-order fractional models have been successfully employed in diverse applications, including the analysis of material microstructures [7], continuum mechanics with variable-order fractional operators [8], nonlinear viscoelasticity [9], and the static response of nonlocal beam structures [10].

The additional mathematical complexity associated with variable-order operators poses significant challenges for analytical treatment, motivating the development of robust and efficient numerical methods. Several strategies have been proposed in recent years. Shen et al. [11] extended the variable-order operator proposed by Coimbra, as formulated in [6], to address time-fractional diffusion equations. Chen et al. [12] developed finite-difference-based schemes for problems involving variable-order derivatives. Cao and Qiu [13] introduced a second-order approximation for variable-order fractional ordinary differential equations formulated with the Riemann–Liouville derivative. Zayernouri and Karniadakis [14] proposed a fractional spectral collocation method for variable-order partial differential equations. Zhao et al. [15] derived second-order approximation formulas for time-fractional derivatives of variable order. Li et al. [16] proposed a high-order numerical scheme for variable-order fractional functional differential equations, while Li and Wu [17] developed a reproducing-kernel-based numerical method for variable-order fractional functional boundary-value problems. Nemati et al. [18] proposed a Bernoulli-polynomial-based approach for solving multi-term variable-order fractional differential equations.

Ayazi et al. [19] developed an adjusted spectral element method for variable-order fractional delay differential equations, using Lagrangian basis functions and variable-order differentiation matrices within individual spectral elements. A penalty technique was employed to control discontinuities at element interfaces, and numerical tests demonstrated accurate and computationally efficient solutions. Derakhshan [20] proposed a shifted Jacobi–Gauss collocation method for coupled differential–integral equations involving variable-order Caputo operators, transforming the original problem into an algebraic system and treating linear and nonlinear cases through appropriate numerical procedures. Ahmed et al. [21] developed a spectral collocation method based on generalized fractional Jacobi functions, with operational matrices for integer- and variable-order fractional derivatives and basis functions that incorporate prescribed initial conditions. Postavaru and Toma [22] introduced a hybrid basis combining block-pulse functions and fractional Fibonacci polynomials for multiterm variable-order fractional equations, using an exact representation of the Riemann-Liouville integral and a Newton–Cotes collocation scheme to obtain the resulting algebraic systems. More recently, Al-Sharif et al. [23] proposed a spectral collocation method based on fractional-order Chelyshkov functions, deriving an exact operational matrix for variable-order fractional integration and demonstrating accurate solutions with a relatively small number of basis functions.

In parallel, fractional modeling has also been explored in electrical engineering applications, particularly in systems composed of resistors (R), inductors (L), and capacitors (C), commonly referred to as Resistor-Inductor-Capacitor (RLC) circuits. Gómez-Aguilar et al. [24] analyzed RC, LC, and RL circuits using the Atangana-Baleanu fractional derivative. Sene and Gómez-Aguilar [25] investigated analytical solutions of fractional-order electrical circuit models. Naveen et al. [26] examined RLC systems described by the Hilfer fractional derivative under nonlocal boundary conditions, whereas Malarvizhi et al. [27] conducted a numerical analysis of an RLC circuit using a fourth-order Runge-Kutta scheme. Naveen and Parthiban [28] investigated LC and RC electrical circuits modeled using a variable-order Caputo fractional derivative. The study analyzed the mathematical properties of the resulting systems and employed modified Euler and fourth-order Runge-Kutta methods for their numerical solution.

The vast majority of studies reported in the literature focus on fractional ordinary differential equations or variable-order fractional partial differential equations. Consequently, the development of numerical methodologies specifically tailored to variable-order fractional algebraic-differential equations remains a significant and recurring research gap.

Motivated by the need for accurate, computationally efficient, and readily extendable techniques to address the inherent complexity of variable-order formulations in an algebraic-differential framework, the present work proposes a novel numerical approach for solving variable-order fractional algebraic-differential equations subject to prescribed

initial conditions. The proposed methodology extends the classical Orthogonal Collocation Method to accommodate time-dependent fractional orders. Its accuracy, robustness, and applicability are demonstrated through three representative case studies, including two benchmark mathematical problems and a classical RLC circuit model.

The remainder of this paper is organized as follows. Section 2 presents the mathematical modeling of the RLC circuit. Section 3 introduces the formulation of fractional algebraic-differential equations. Section 4 briefly reviews relevant definitions of fractional derivatives. Section 5 details the proposed numerical methodology. Section 6 discusses the numerical results for both case studies. Finally, the concluding section summarizes the main findings and outlines directions for future research.

2. RLC circuit

An RLC circuit is a fundamental system in electrical engineering composed of four elements: a resistor (R), an inductor (L), a capacitor (C), and a voltage source (E). These components may be connected in series or in parallel, forming a system that exhibits resistive, inductive, and capacitive behaviors [29]. The resistor dissipates energy as heat, the inductor stores energy in the magnetic field generated by the current, and the capacitor stores energy in the electric field between its plates. The interaction among these elements results in a dynamic system capable of oscillatory behavior.

The current and voltage dynamics of an RLC circuit are governed by a second-order differential equation derived from Kirchhoff's laws. Depending on the damping ratio, the circuit response can be classified as underdamped, overdamped, or critically damped [29].

According to Kirchhoff's voltage law, the sum of voltage drops in a closed RLC circuit is equal to the applied voltage. This yields the following second-order ordinary differential equation with initial conditions:

$$L\frac{d^2Q(t)}{dt^2} + R\frac{dQ(t)}{dt} + \frac{1}{C}Q(t) = E(t) \tag{1}$$

$$Q(0) = q_0 \tag{2}$$

$$\frac{dQ(0)}{dt} = I_0, \tag{3}$$

where t denotes time, $Q(t)$ is the charge on the capacitor, $I(t) = dQ(t)/dt$ is the circuit current, q_0 is the initial charge, and I_0 is the initial current.

3. Variable-order fractional algebraic-differential equation system

In this work, a system of Fractional Algebraic-Differential Equations (FADEs) is considered, in which the classical integer-order derivative ($\alpha = 1$) is replaced by the Caputo fractional derivative [30], where the fractional order α is allowed to vary with time. The system is expressed as follows:

$$D^{\alpha(t)}x(t) = f\big(t,\, x(t),\, y(t)\big), \quad x(0) = x_0 \tag{4}$$

$$0 = g\big(t,\, x(t),\, y(t)\big), \quad y(0) = y_0, \tag{5}$$

where $x(t)$ and $y(t)$ denote the vectors of differential and algebraic variables, respectively; $x(0)$ and $y(0)$ are the corresponding initial condition vectors; f and g are known analytical functions; and $\alpha(t)$ denotes the variable fractional order.

Analytical solutions to this class of systems are, in general, difficult or unavailable. Consequently, numerical approximation techniques are required and are addressed in Section 5.

4. Fractional derivatives

In this section, classical approximations used to evaluate fractional operators found in FADEs are revisited [30].

4.1 *Definition 1*

The Riemann-Liouville type fractional integral ($I^{\alpha}F(t)$) of order $\alpha(\alpha > 0)$ applied to a generic function F defined on the set of positive real numbers is given by:

$$I^{\alpha}F(t) = \frac{1}{\Gamma(\alpha)} \int_0^t (t-\tau)^{\alpha-1} F(\tau) d\tau, \tag{6}$$

where Γ denotes the Gamma function.

4.2 *Definition 2*

The Riemann-Liouville type fractional derivative (${}_{\mathrm{RL}}D^{\alpha}F(t)$) of order α ($\alpha > 0$) applied to a generic function F defined on the set of positive real numbers is given by:

$${}_{\mathrm{RL}}D^{\alpha}F(t) = \frac{d^n}{dt^n} \frac{1}{\Gamma(n-\alpha)} \int_0^t (t-\tau)^{n-\alpha-1} F(\tau) d\tau, \tag{7}$$

where $n = [\alpha] + 1$ and $[\alpha]$ is an operator that represents the integer part of α.

4.3 *Definition 3*

The Caputo type fractional derivative (${}_{\mathrm{C}}D^{\alpha}F(t)$) of order α ($\alpha > 0$) applied to a generic function F defined on the set of positive real numbers is given by:

$${}_{\mathrm{C}}D^{\alpha}F(t) = \frac{1}{\Gamma(n-\alpha)} \int_0^t (t-\tau)^{n-\alpha-1} F^{(n)}(\tau) d\tau, \tag{8}$$

where $n = [\alpha] + 1$ and $[\alpha]$ is an operator that represents the integer part of α.

4.4 *Definition 4*

The Shifted Grunwald fractional derivative (${}_{\mathrm{S}}D^{\alpha}F(t)$) of order α ($1 < \alpha < 2$) applied to a generic function F defined on the set of positive real numbers is given by:

$$ {}_{S}D^{\alpha}F(t) = \frac{1}{h^{\alpha}} \sum_{k=0}^{M} \left((-1)^{k} \frac{\Gamma(\alpha+1)}{\Gamma(k+1)\Gamma(\alpha-k+1)} \right) F\big(x-(k-1)h\big), \tag{9} $$

where M is the number of discretization points and $h = (t_f - t_0)/M$ is the integration step (t_0 and t_f represent the initial and final times, respectively).

4.5 *Definition 5*

If f is a continuous function with fractional order equal to $k\alpha$ (where k is a positive integer and $1 < \alpha < 2$), the fractional Taylor expansion for this function is written as follows:

$$ F(t+h) = \sum_{k=0}^{\infty} \frac{h^{k\alpha}}{\Gamma(1+k\alpha)} F^{k\alpha}(t). \tag{10} $$

5. Methodology

The proposed methodology was developed to solve initial-value variable-order fractional algebraic-differential systems. The main idea consists of approximating the unknown state variables through polynomial interpolation and enforcing the governing equations at a set of collocation points, thereby transforming the original problem into a system of nonlinear algebraic equations.

Let $\Theta(x)$ be a continuous function defined over a given interval and approximated by:

$$ \Theta(x) \approx \sum_{j=1}^{\kappa} \beta_j P_j(x), \tag{11} $$

where κ denotes the polynomial degree, $P_j(x)$ are the Lagrange interpolation polynomials, and β_j are the unknown coefficients to be determined.

To represent the fractional dynamics, the variable-order Caputo derivative of a generic polynomial ($P_j(x)$) is considered. For a constant fractional order α, the Caputo derivative is defined in terms of the Riemann–Liouville fractional integral of the integer-order derivative. Following the formulation adopted by Naveen and Parthiban [31], extending this definition to a variable order $\alpha(x)$ yields:

$$ {}_{C}D^{\alpha(x)}P_j(x) = \frac{1}{\Gamma(m-\alpha(x))} \int_{0}^{x} (x-\tau)^{m-\alpha(x)-1} P_j^{m}(\tau)\, d\tau, \quad m-1 < \alpha(x) < m. \tag{12} $$

Using this operator, the right-hand side of Eq. (4) can be approximated as:

$$ F\big(x,\ \alpha(x),\ \Theta(x),\ \Theta(g(x))\big) \approx F\left(x,\ \alpha(x),\ \sum_{j=1}^{\kappa} \beta_j P_j(x),\ \sum_{j=1}^{\kappa} \beta_j P_j(g(x))\right). \tag{13} $$

Substituting the polynomial approximation into the governing equation leads to the definition of the residual function (R_{es}):

$$R_{es} = \sum_{j=1}^{\kappa} \beta_j D^{\alpha} P_j(x) - F\left(x,\ \alpha(x),\ \sum_{j=1}^{\kappa} \beta_j P_j(x),\ \sum_{j=1}^{\kappa} \beta_j P_j(g(x))\right). \tag{14}$$

The collocation strategy requires the residual to vanish at a finite set of discrete points. In this work, the collocation points are selected as the Jacobi–Gauss–Radau nodes [32]. Furthermore, the initial condition is directly imposed at the first collocation point ($x_i = 0$) according to:

$$\sum_{j=1}^{\kappa} \beta_j P_j(0) = \Theta_0. \tag{15}$$

The same procedure can be applied to approximate the algebraic function $g(t,\ x(t),\ y(t))$ appearing in Eq. (5). Consequently, the original variable-order fractional algebraic–differential system is converted into a coupled system of $2\kappa+1$ nonlinear algebraic equations with $2\kappa+1$ unknown coefficients.

The Caputo fractional derivative is adopted in this work because it naturally incorporates memory effects through a convolution between an integer-order derivative and a power-law kernel. An additional advantage is that the associated initial conditions can be prescribed in a manner similar to those used for classical integer-order differential equations [30]. In this work, the fractional order is allowed to vary with time, leading to the variable-order fractional algebraic-differential system considered herein.

The overall computational procedure can be summarized as follows:

1. Define the mathematical model, including the variable-order fractional algebraic–differential equations, the initial conditions, the approximation order (N) (yielding $(N+1)$ unknown coefficients), and the orthogonal polynomial used to generate the collocation points.

2. Compute the Jacobi–Gauss–Radau collocation points.

3. Construct the Lagrange interpolation polynomials associated with the collocation nodes and approximate the unknown state variables.

4. Evaluate the variable-order Caputo derivative of the approximation functions and substitute the resulting expressions into the original governing equations.

5. Formulate the residual equations and enforce their satisfaction at the collocation points while simultaneously imposing the prescribed initial conditions.

6. Solve the resulting algebraic system using the Newton method for nonlinear problems or Lower-Upper (LU) decomposition for linear systems.

7. Assess the convergence of the numerical solution by progressively increasing the approximation order and verifying the sensitivity of the results.

It is important to emphasize that the Jacobi–Gauss–Radau collocation points were selected because they naturally include a boundary point of the domain, thereby facilitating the direct enforcement of initial conditions in initial-value problems [32]. In addition, the accuracy of the proposed approach depends on both the approximation basis and the number of collocation points employed. Increasing the polynomial degree does not necessarily lead to improved accuracy, as excessive refinement may introduce numerical oscillations or lead to ill-conditioning.

6. Results and discussion

6.1 *Mathematical applications*

To validate the proposed methodology and assess the influence of the number of collocation points ($N = \kappa+1$), this subsection presents mathematical case studies.

The first case considers the following variable-order fractional differential–algebraic equation with fractional order $\alpha(t)$ [33]:

$$D^{\alpha(t)}x(t) = -2x(t) + y(t) + f(t), \quad x(0) = 0, \tag{16}$$

$$0 = x(t) + y(t) - t^2 - \exp(-t), \quad y(0) = 1, \tag{17}$$

where t is the independent variable defined over the interval $[0,\ 1]$, and $x(t)$ and $y(t)$ denote the differential and algebraic dependent variables, respectively. The function $f(t)$ is selected such that the exact solution of the problem, independently of $\alpha(t)$, is given by $x(t) = t^2$ and $y(t) = \exp(-t)$.

Table 1 reports the sums of the mean squared errors obtained using the Orthogonal Collocation Method for different values of N and three functional representations of $\alpha(t)$, namely, $1/(1+\exp(-t))$, $1-\exp(t)\cos(t)/10$, and $1-0.5t$, as well as the classical integer-order case. The obtained results are compared with both the results reported in Mortezaee et al. [33] and those generated using the Adams-type Predictor–Corrector Method (APCM), considering 250 discretization points.

Table 1. Sum of the mean squared error considering the Orthogonal Collocation Method for the first mathematical application

	$\alpha(t)$			
N	1	$1/(1+\exp(-t))$	$1-\exp(t)\cos(t)/10$	$1-0.5t$
2	1.2858×10^{-18}	3.4420×10^{-17}	8.3122×10^{-19}	2.5588×10^{-18}
3	2.8648×10^{-16}	1.7196×10^{-16}	1.4458×10^{-17}	1.8481×10^{-16}
4	4.1543×10^{-15}	2.3711×10^{-14}	1.2576×10^{-15}	3.0747×10^{-15}
5	1.2128×10^{-13}	2.9600×10^{-13}	2.4794×10^{-14}	4.3182×10^{-13}
APCM	2.8543×10^{-8}	8.5454×10^{-9}	1.4334×10^{-8}	3.4545×10^{-8}
[33]	1.0588×10^{-6}	1.1053×10^{-6}	1.0720×10^{-6}	8.5192×10^{-7}

As shown in Table 1, the method consistently produced highly accurate solutions for all variable-order functions considered, with the sum of the mean squared errors remaining between 10^{-18} and 10^{-13}. Such results demonstrate the robustness of the proposed formulation, even when the fractional order varies significantly throughout the computational domain.

A noteworthy aspect is that the smallest errors were obtained with only two collocation points ($N = 2$). This behavior is directly associated with the analytical solution of the problem, since $x(t) = t^2$ is a quadratic polynomial. In this particular case, the approximation space generated by a quadratic interpolation is already capable of reproducing the exact solution with machine-level precision. Consequently, increasing the number of collocation points does not provide additional benefits and may even introduce a slight accumulation of numerical round-off errors, which explains the marginal increase observed for larger values of N.

The observed behavior suggests that the benchmark solution lies within the approximation space generated by the collocation basis. Consequently, increasing the polynomial degree does not improve the approximation error and may amplify round-off effects due to the solution of increasingly ill-conditioned algebraic systems.

When compared with the results reported by Mortezaee et al. [33], the superiority of the proposed approach becomes evident. While the errors reported in the literature are predominantly of the order of 10^{-6}, the present methodology reduced the error magnitude by approximately twelve orders of magnitude, reaching values close to machine precision. Similar conclusions can be drawn from the comparison with the APCM. Although APCM provided satisfactory approximations,

with errors around 10^{-8} and 10^{-9}, the Orthogonal Collocation Method still achieved substantially greater accuracy, indicating its enhanced capability for solving variable-order fractional differential-algebraic systems.

Figure 1 shows the variable-order function, the resulting solution profiles, and the corresponding absolute error obtained for the first benchmark problem using two collocation points.

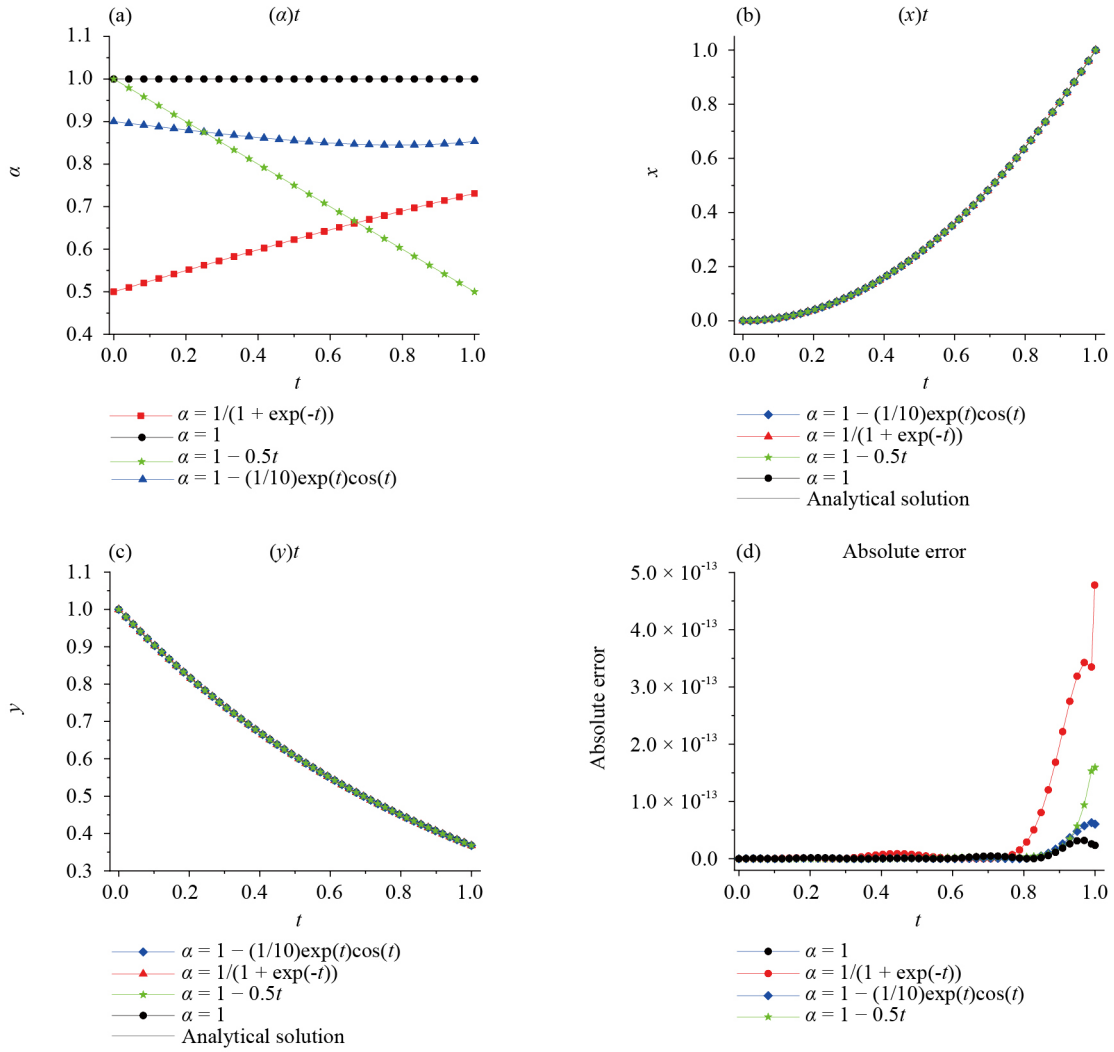


Figure 1. Profiles of the variable fractional order, dependent variables, and absolute error of the first mathematical function with two collocation points

In this figure, the numerical solutions for both $x(t)$ and $y(t)$ are visually indistinguishable from the analytical solution throughout the entire integration interval, regardless of the selected fractional-order function (see Figures 1b and 1c). The absolute error also remains extremely small over most of the time domain, reaching its highest values only near the end of the simulation (see Figure 1d). This behavior is commonly observed in initial-value problems, where local discretization errors gradually accumulate as the integration progresses. In fractional-order systems, this effect deserves particular attention because the memory property inherent in fractional derivatives can influence the solution over extended time intervals and, consequently, affect long-term or steady-state predictions. In the present case, however, the increase in absolute error near the end of the time interval does not alter the overall behavior of the numerical solution, which remains in good agreement with the reference solution. Therefore, within the time interval investigated, the observed error accumulation does not compromise the reliability of the results.

From a computational standpoint, the proposed method also demonstrates favorable performance. Executed on an Intel i7 processor with 8 GB of RAM, the average computational time was below 2 s, whereas the APCM required approximately 6 s under the same conditions. Therefore, beyond its remarkable accuracy, the Orthogonal Collocation Method also offers a significant reduction in computational cost, making it an attractive alternative for the numerical treatment of variable-order fractional differential-algebraic equations.

The second case considers a variable–order fractional differential-algebraic equation with fractional order $\alpha(t)$ defined as [33]:

$$D^{\alpha(t)}x(t) = t\frac{dy(t)}{dt} - x(t) + (1+t)y(t), \quad x(0) = 1, \tag{18}$$

$$0 = y(t) - \sin(t), \quad y(0) = 0, \tag{19}$$

where t is the independent variable defined over the interval $[0,\ 1]$, and $x(t)$ and $y(t)$ denote the differential and algebraic dependent variables, respectively.

Table 2 presents the absolute errors of $y(t)$ for $\alpha(t) = 1 - \cos(t)^2/2$ considering the proposed methodology and the reported results obtained by Mortezaee et al. [33] and using the APCM, considering 250 discretization points. The obtained results demonstrate that the Orthogonal Collocation Method maintained a high level of accuracy over the entire temporal domain, with errors predominantly ranging from 10^{-12} to 10^{-10}. These values indicate that the numerical approximation remains highly stable even in the presence of nonlinear variable-order effects.

Table 2. The absolute errors of $y(t)$ considering the Orthogonal Collocation Method for the second mathematical application

	$\alpha(t) = 1 - \cos(t)^2/2$				
N	$t = 0.2$	$t = 0.4$	$t = 0.6$	$t = 0.8$	$t = 1.0$
2	0.6434×10^{-12}	0.6845×10^{-12}	0.6977×10^{-12}	0.8333×10^{-12}	0.9343×10^{-10}
3	0.1433×10^{-11}	0.2636×10^{-12}	0.3434×10^{-12}	0.4655×10^{-12}	0.9899×10^{-10}
4	0.2433×10^{-11}	0.5223×10^{-11}	0.5733×10^{-11}	0.6666×10^{-12}	0.8345×10^{-10}
5	0.4574×10^{-12}	0.5630×10^{-11}	0.6976×10^{-11}	0.7670×10^{-11}	0.7698×10^{-11}
APCM	0.2434×10^{-7}	0.6435×10^{-7}	0.9786×10^{-8}	0.5655×10^{-8}	0.8994×10^{-8}
[33]	8.1988×10^{-6}	2.1679×10^{-6}	1.6166×10^{-5}	2.7206×10^{-5}	4.2586×10^{-5}

Unlike the first application, where the solution could be represented exactly by a low-order polynomial approximation, the second problem involves more complex dynamic behavior. Even so, the collocation framework accurately captured the solution characteristics using a relatively small number of collocation points. The results obtained for $N = 5$ were particularly noteworthy, yielding errors consistently close to machine precision throughout the investigated interval.

The errors reported by Mortezaee et al. [33] lie between 10^{-6} and 10^{-5}, whereas the present methodology reduced these discrepancies by approximately five to seven orders of magnitude. Likewise, although the APCM generated acceptable results with errors around 10^{-7} and 10^{-8}, the Orthogonal Collocation Method achieved a substantially higher degree of accuracy at all evaluation points.

Figure 2 presents the variable-order functions investigated, namely, $\alpha(t) = 1$, $\alpha(t) = 1 - 0.5/(1+\exp(-t))$, $\alpha(t) = 1 - \exp(t)\cos(t)/10$, $\alpha(t) = \tanh(t+1)$, and $\alpha(t) = 1 - \cos(t)^2/2$, together with the corresponding numerical results obtained using five collocation points. For the integer-order case, i.e., $\alpha(t) = 1$, the exact analytical solution is given by $x(t) = \exp(-t) + t\sin(t)$ and $y(t) = \sin(t)$.

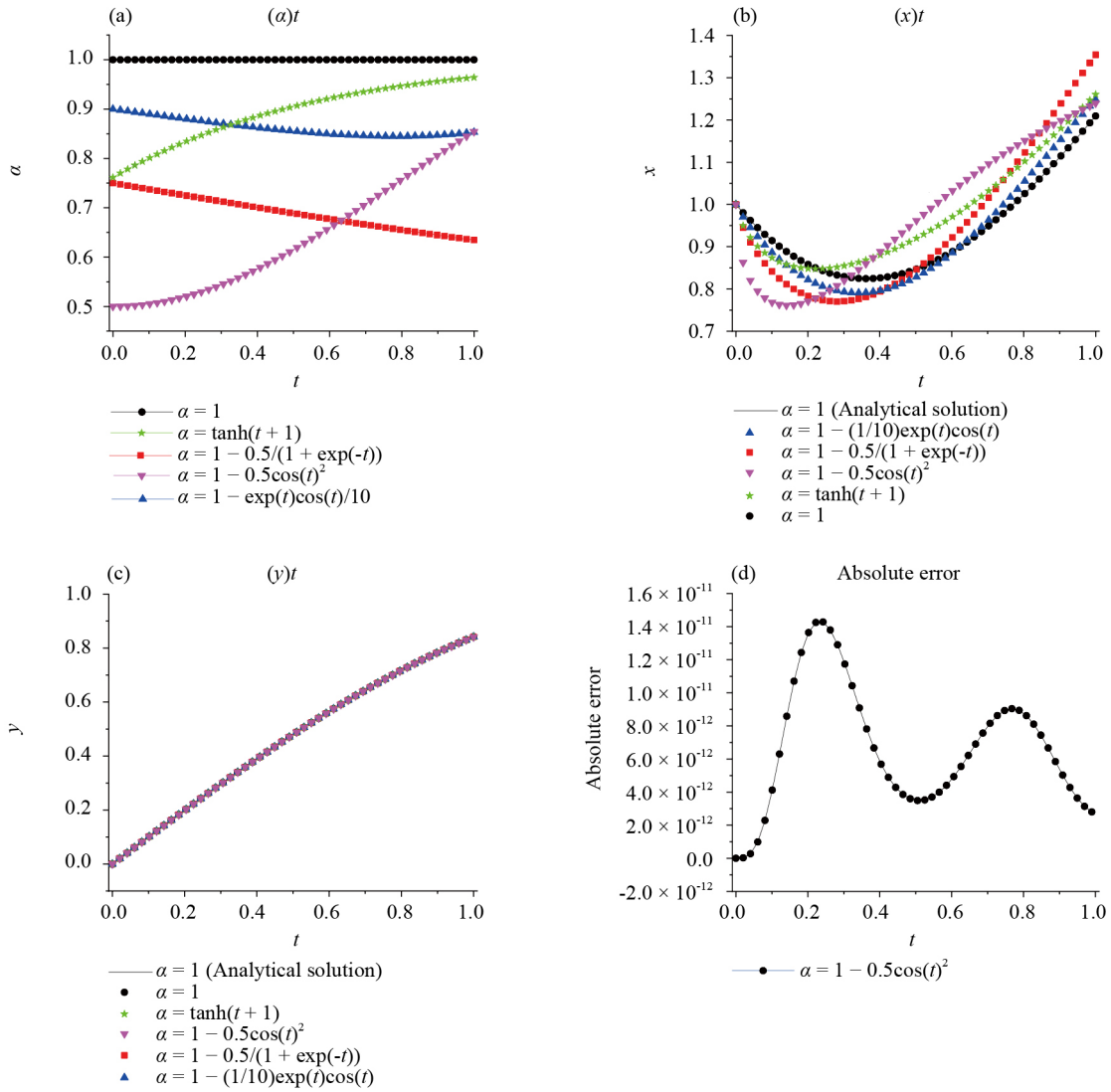


Figure 2. Profiles of the variable fractional order, dependent variables, and absolute error of the second mathematical function with five collocation points

The graphical results shown in Figures 2b and 2c reinforce these quantitative findings. The predicted profiles of both state variables exhibit smooth behavior and remain fully consistent with the expected physical dynamics of the system. Furthermore, the absolute error associated with the fractional-order case $\alpha(t) = 1 - \cos(t)^2/2$ remains extremely small throughout the simulation, confirming the numerical reliability of the proposed formulation (see Figure 2d).

Computational efficiency was also preserved in this second application. The average processing time was approximately 3 s, compared with about 5 s required by the APCM. This reduction in computational effort, combined with the significant improvement in accuracy, demonstrates that the proposed Orthogonal Collocation Method provides an effective balance between precision and computational cost. Overall, the results obtained in both benchmark problems indicate that the methodology constitutes a competitive and reliable numerical framework for solving variable-order fractional differential-algebraic equations, particularly when high-accuracy solutions are required.

6.2 *RLC circuit*

In this application, the dynamic behavior of the RLC circuit is analyzed under both free-response ($E(t) = 0$) and forced-response ($E(t) \neq 0$) conditions. For this purpose, the following cases are investigated. The first corresponds to the underdamped regime ($R < R_c \approx (4L/C)^{0.5}$), which is analogous to the simple harmonic motion of an undamped mass-spring system. The second case addresses the critically damped regime ($R = R_c$), while the third considers the overdamped regime ($R > R_c$). In all simulations, five collocation points were employed, based on preliminary numerical tests.

To apply the proposed methodology to the RLC circuit with variable fractional order, the original second-order model is first rewritten as a system of first-order differential equations. Subsequently, the integer-order derivatives are replaced by variable-order fractional derivatives $\alpha(t)$, yielding:

$$\frac{1}{\sigma^{(1-\alpha(t))}} \frac{d^{\alpha(t)} Q(t)}{dt^{\alpha(t)}} = I(t) \tag{20}$$

$$\frac{1}{\sigma^{(1-\alpha(t))}} \frac{d^{\alpha(t)} I(t)}{dt^{\alpha(t)}} = -\frac{R}{L} I(t) - \frac{Q(t)}{CL} + \frac{E(t)}{L} \tag{21}$$

$$E(t) = 0 \text{ or } E(t) \neq 0 \tag{22}$$

$$Q(0) = q_0 \tag{23}$$

$$\frac{dQ(0)}{dt} = I_0, \tag{24}$$

where t denotes time, $I(t)$ is the circuit current, $Q(t)$ is the capacitor charge, and q_0 and I_0 are the initial charge and current, respectively. The parameter σ, which has units of time, was introduced to ensure the dimensional consistency of the fractional phenomenological model. This modification guarantees that the fractional differential operator remains dimensionally consistent. In addition, to prevent this parameter from quantitatively influencing the simulated profiles, it is set equal to unity.

It is important to emphasize that the same variable-order derivative was adopted in both state equations to represent a global memory mechanism affecting the overall circuit dynamics. Although more sophisticated formulations may assign distinct fractional orders to each energy-storage element, the present choice was made to isolate and evaluate the impact of a single variable-order memory parameter.

For simulation purposes, the following parameters are considered: $R = 40\ \Omega$, $L = 0.2$ H, and $C = 10^{-4}$ F, with initial conditions $q_0 = 2$ C and $I_0 = 0$ A. Under these conditions, the critical resistance is $R_c = 89.4427\ \Omega$. Thus, to evaluate the underdamped, critically damped, and overdamped responses, the resistance values $R = 10\ \Omega$, $R = 89.4427\ \Omega$, and $R = 200\ \Omega$ are adopted, respectively. The RLC circuit model was simulated up to a final time of $t_f = 0.5$ s using the proposed methodology.

To assess the impact of the fractional order on the current dynamics of the RLC circuit, four representative variable-order functions are studied: $\alpha(t) = 1$; $\alpha(t) = 0.4 + 0.6/(1 + \exp(-4t))$; $\alpha(t) = 0.8 + 0.1\cos(4t)$ and $\alpha(t) = 0.7 + 0.3t$. Together, these functions capture distinct memory regimes, ranging from nearly integer-order behavior to time-dependent increasing, oscillatory, and decreasing memory effects.

It is worth noting that the functions adopted in this study are derived from those originally proposed by Mortezaee et al. [33]. The parameters were modified to constrain the fractional order to the interval $[0.7,\ 1]$, as illustrated in Figure 3. This modification was introduced for two main reasons. First, it avoids fractional-order values below 0.5 or above unity over the simulation interval, as such values may lead to responses that are not physically meaningful for the case study

considered. Second, it enables a more reliable assessment of the effect of the fractional order on the system dynamics, emphasizing its influence on the physical variables while minimizing the effects associated with very low values of $\alpha(t)$.

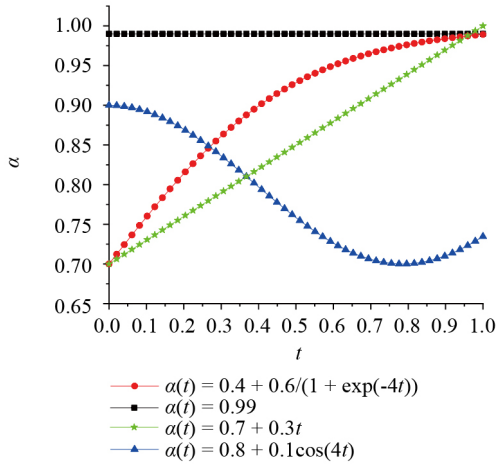


Figure 3. Comparison of the variable-order fractional functions $\alpha(t)$ adopted in the RLC circuit model

To complement the analysis of the current evolution and to quantitatively characterize the distinct dynamical behaviors observed in the circuit, several metrics grounded in energy-based considerations and fractional-memory effects are employed. These measures quantify the energy dissipated within the resistive element, the energy delivered by the external source, the energetic efficiency of the system, and the extent to which fractional memory influences the electrical response. The mathematical definitions and physical interpretations of these metrics are presented below [34], [35].

• Dissipated energy in the resistor (W_R): This quantity represents the cumulative electrical energy irreversibly dissipated as heat within the resistive element during the simulation period. As the dissipated power is proportional to $I(t)^2$, higher values of W_R are associated with a larger current circulation over time and, consequently, stronger energy losses. It is mathematically expressed as:

$$W_R = \int_0^{t_f} R_c I(t)^2 dt. \tag{25}$$

• Net energy supplied by the source (W_E): This quantity represents the net electrical work performed by the external source on the circuit over the simulation interval. It is calculated as the time integral of the instantaneous power supplied by the source, $E(t)I(t)$. Therefore, W_E is expressed in joules (J) and may be positive or negative, depending on the direction of net energy transfer. Positive values indicate net energy supplied to the circuit, whereas negative values indicate net energy returned from the circuit to the source. Mathematically, it can be expressed as:

$$W_E = \int_0^{t_f} E(t)I(t)dt. \tag{26}$$

Therefore, when $E(t) = 0$, the energy supplied by the source is identically zero, leading to $W_E = 0$. In contrast, under constant or time-varying excitations, such as sinusoidal inputs, this metric quantifies the net electrical work performed by the external source on the circuit over the considered time interval. Consequently, W_E provides a direct measure of the

net energy transferred between the external source and the circuit, thereby quantifying the net energetic contribution of the source to the system dynamics.

• Dissipation ratio (η): This metric represents the fraction of the total energy available in the system that is ultimately dissipated by the resistive element. It provides an indication of how effectively the energy introduced into the circuit is converted into irreversible losses, rather than being temporarily stored in the inductive and capacitive components. Mathematically, it is defined as:

$$\eta = 100\frac{W_R}{W_R + W_L + W_C}, \tag{27}$$

where W_R is defined by Eq. (25), while W_L and W_C denote the energies stored in the inductor and capacitor, respectively. These quantities are given by:

$$W_L = 0.5LI(t_f)^2 \tag{28}$$

$$W_C = \frac{Q(t_f)^2}{2C}. \tag{29}$$

When all the energy available in the system has been converted into heat, the stored energy contributions become negligible, i.e., $W_L \approx 0$ and $W_C \approx 0$, yielding $\eta \approx 1$ (or 100%). Conversely, when a substantial portion of the energy remains stored in the reactive elements, such that the combined stored energy $W_L + W_C$ is much larger than the energy dissipated by the resistor W_R, the efficiency approaches zero. In this situation, energy is predominantly exchanged between the magnetic field of the inductor and the electric field of the capacitor, while only a small fraction is irreversibly dissipated. Therefore, higher values of η indicate a strongly dissipative response, whereas lower values are characteristic of a more conservative and oscillatory regime, in which energy storage and exchange dominate the circuit dynamics.

• Memory index (I_M): This metric quantifies the overall deviation between the fractional-order model and its integer-order counterpart over the entire simulation interval. It provides a global measure of the influence of memory effects introduced by the fractional formulation on the system dynamics. Larger values of I_M indicate a stronger departure from the classical integer-order behavior, whereas values close to zero suggest that the fractional model exhibits a response similar to that of the conventional model. Mathematically, the memory index is defined as:

$$I_M = \frac{\sqrt{\int_0^{t_f} \left(I^{\alpha}(t) - I^{1}(t)\right)^2 dt}}{\sqrt{\int_0^{t_f} \left(I^{1}(t)\right)^2 dt}}, \tag{30}$$

where $I^{\alpha}(t)$ and $I^{1}(t)$ represent the current responses obtained from the fractional-order and classical integer-order formulations, respectively.

• Energy dissipation variation (ΔW_R): This metric quantifies the relative change in the energy dissipated by the resistor resulting from the adoption of a fractional-order formulation. It provides a direct assessment of how memory effects influence the circuit's dissipative behavior when compared with the corresponding integer-order model. Positive values of ΔW_R indicate an increase in energy dissipation, whereas negative values reflect a reduction in the amount of energy converted into heat. Mathematically, the metric is defined as:

$$\Delta W_R = 100\frac{\Delta W_R(\alpha) - \Delta W_R(1)}{\Delta W_R(1)}, \tag{31}$$

where $\Delta W_R(\alpha)$ and $\Delta W_R(1)$ correspond to the energies dissipated by the fractional-order and classical integer-order models, respectively.

The corresponding quantitative results are summarized in Table 3, which compares the dissipated energy (W_R), supplied energy (W_E), dissipation ratio (η), memory index (I_M), and energy deviation (ΔW_R) for the fractional RLC models considered. The analysis includes different fractional-order functions, $\alpha(t)$, three resistance values (R_c = 10, 89.4427, and 200 Ω), and three external excitation scenarios, namely $E(t) = 0$, $E(t) = 5{,}000$ V, and $E(t) = 5{,}000\sin(50t)$ V.

Focusing first on the effect of the resistance, the case with $R_c = 10$ Ω exhibits pronounced transient oscillations with relatively large amplitudes, followed by rapid attenuation. This behavior is typical of weakly resistive RLC circuits, where energy is repeatedly exchanged between the inductor and the capacitor before being dissipated through the resistor. As the resistance increases to $R_c = 89.4427$ Ω and subsequently to $R_c = 200$ Ω, the transient oscillations become progressively less pronounced and the overall response becomes increasingly damped. Nevertheless, under sinusoidal excitation, periodic oscillations persist even at the highest resistance values, reflecting the continuous energy input provided by the external source.

Table 3. Performance metrics of the fractional RLC circuit under different fractional orders, resistance values, and excitation conditions (E_1 = 0 V, E_2 = 5,000 V and E_3 = 5,000 sin(50t) V)

	$\alpha(t) = 1$								
	$R_c = 10$ Ω			$R_c = 89.4427$ Ω			$R_c = 200$ Ω		
	E_1 (V)	E_2 (V)	E_3 (V)	E_1 (V)	E_2 (V)	E_3 (V)	E_1 (V)	E_2 (V)	E_3 (V)
W_R (J)	18,195.72	10,235.08	19,434.59	19,791.94	11,132.96	27,805.84	19,913.93	11,201.58	30,062.28
W_E (J)	0.00	-7,500.00	1,422.88	0.00	-7,500.00	8,435.91	0.00	-7,500.00	10,617.07
η	100.00	89.11	99.41	100.00	89.90	98.68	100.00	89.96	98.55
I_M	-	-	-	-	-	-	-	-	-
ΔW_R	-	-	-	-	-	-	-	-	-
	$\alpha(t) = 0.4 + 0.6/(1 + \exp(-4t))$								
W_R (J)	2,829.85	1,591.79	4,061.17	3,409.12	1,917.63	12,239.44	4,422.21	2,487.49	16,608.86
W_E (J)	0.00	-6,370.36	950.90	0.00	-6,327.14	8,795.49	0.00	-6,291.64	12,163.59
η	99.99	55.94	97.45	99.97	59.75	97.30	99.92	64.88	97.81
I_M	1.07	1.07	1.03	0.94	0.94	0.76	0.76	0.76	0.57
ΔW_R	-85.84	-85.84	-80.85	-82.95	-82.95	-56.31	-77.88	-77.88	-44.93
	$\alpha(t) = 0.8 + 0.1\cos(4t)$								
W_R (J)	11,520.95	6,480.53	12,848.94	12,490.22	7,025.74	20,468.10	13,337.58	7,502.38	23,382.79
W_E (J)	0.00	3,921.04	499.16	0.00	1,663.01	7,900.89	0.00	36.82	10,478.75
η	99.89	85.04	98.44	99.74	87.66	97.07	99.48	89.76	96.56
I_M	1.21	1.21	1.18	0.49	0.49	0.39	0.39	0.39	0.29
ΔW_R	-42.35	-42.36	-39.41	-37.55	-37.55	-26.93	-33.31	-33.31	-22.48
	$\alpha(t) = 0.7 + 0.3t$								
W_R (J)	2,821.20	1,586.92	4,006.86	3,218.81	1,810.58	11,766.63	4,022.85	2,262.85	15,963.33
W_E (J)	0.00	-5,076.19	1,004.91	0.00	-5,025.98	8,581.12	0.00	-5,006.06	11,962.21
η	99.98	55.78	97.48	99.94	57.98	97.29	99.84	62.06	97.86
I_M	1.07	1.07	1.04	0.94	0.94	0.77	0.77	0.77	0.58
ΔW_R	-85.88	-85.88	-81.10	-83.90	-83.90	-57.99	-79.88	-79.88	-47.07

The highest values of the memory index (I_M) are associated with $\alpha(t) = 0.8 + 0.1\cos(4t)$, reaching approximately $I_M = 1.21$ for $R_c = 10\ \Omega$. Although the dissipated energy remains relatively high in this case, the temporal evolution of the current differs substantially from that predicted by the classical integer-order model. On the other hand, increasing the resistance systematically reduces the values of I_M, which decrease to approximately 0.29 when $R_c = 200\ \Omega$. This trend suggests that stronger resistive damping tends to suppress the observable effects of fractional memory on the circuit response.

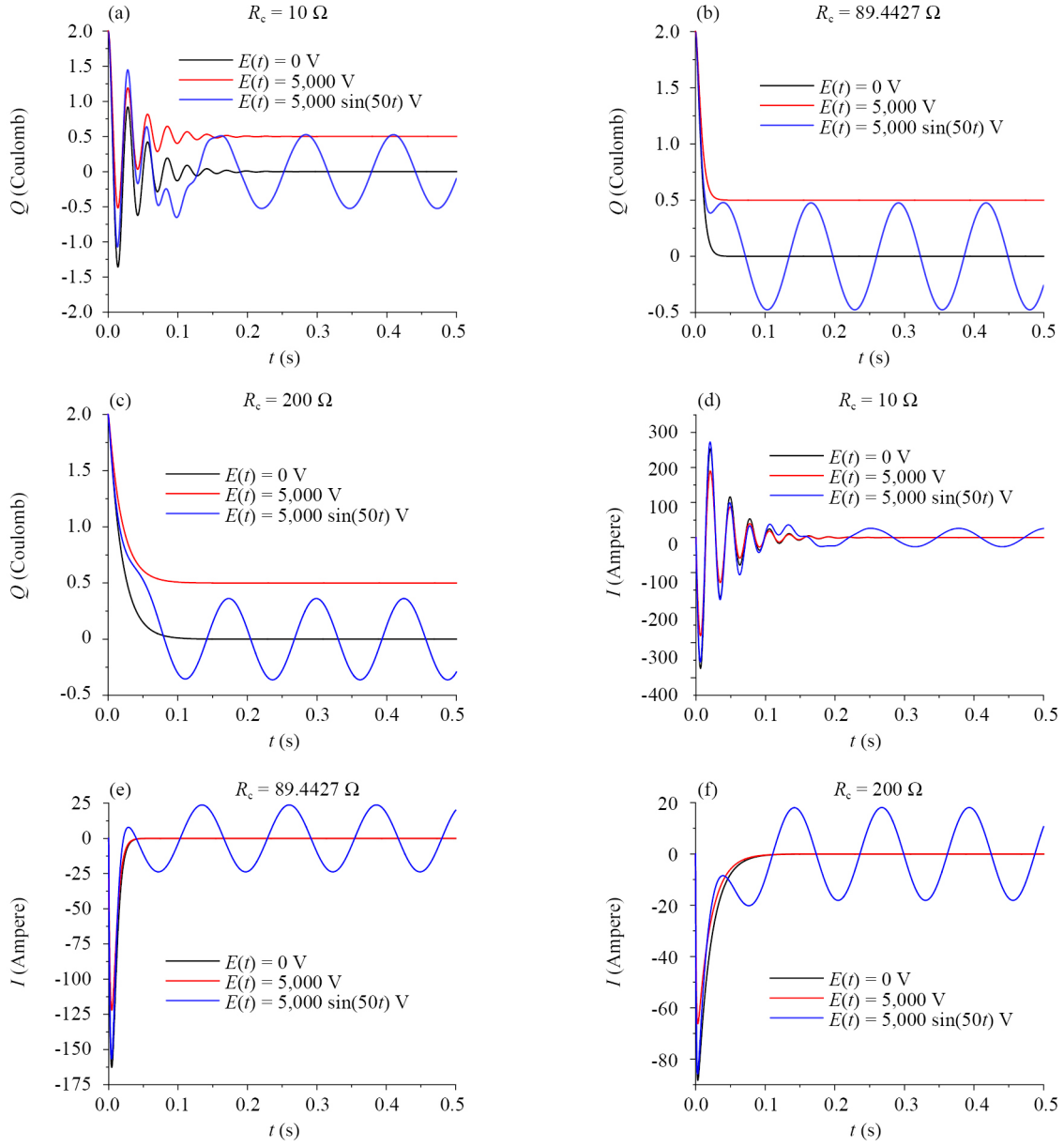


Figure 4. Time-domain current and charge responses of the fractional RLC circuit for a fractional order equal to unity, considering different resistance values and external excitations with five collocation points

The energy dissipation variation (ΔW_R) further quantifies the reduction in dissipation introduced by the fractional-order formulations. For all analyzed cases, negative values are obtained, indicating that the fractional models dissipate less energy than their integer-order counterpart. The most pronounced reductions occur for $\alpha(t) = 0.4 + 0.6/(1 + \exp(-4t))$

and $\alpha(t) = 0.7 + 0.3t$, where the dissipated energy decreases by as much as approximately 86%. These results demonstrate that fractional memory effectively limits current circulation within the circuit and, as a direct consequence, reduces the amount of energy converted into heat through resistive losses.

Figures 4–7 illustrate the current and charge responses as functions of time for different fractional-order functions under the scenarios described earlier. Overall, the results demonstrate that the transient and long-term dynamics of the RLC circuit are strongly affected by both the electrical resistance and the adopted fractional-order formulation. Moreover, the nature of the external excitation plays a decisive role in shaping the long-term system response, with particularly pronounced effects observed under sinusoidal excitation.

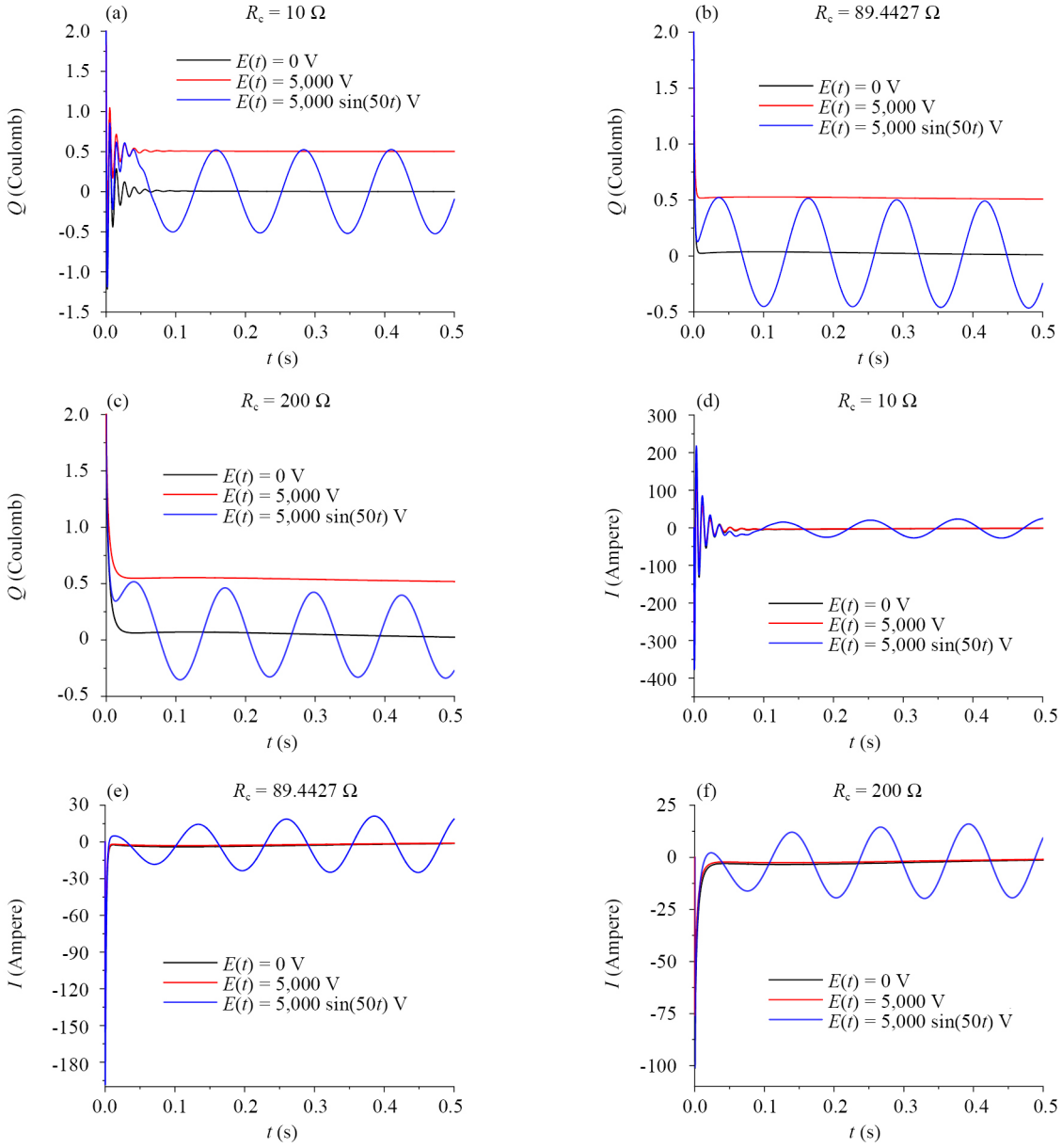


Figure 5. Time-domain current and charge responses of the fractional RLC circuit for a fractional order equal to $0.4 + 0.6/(1 + \exp(-4t))$, considering different resistance values and external excitations with five collocation points

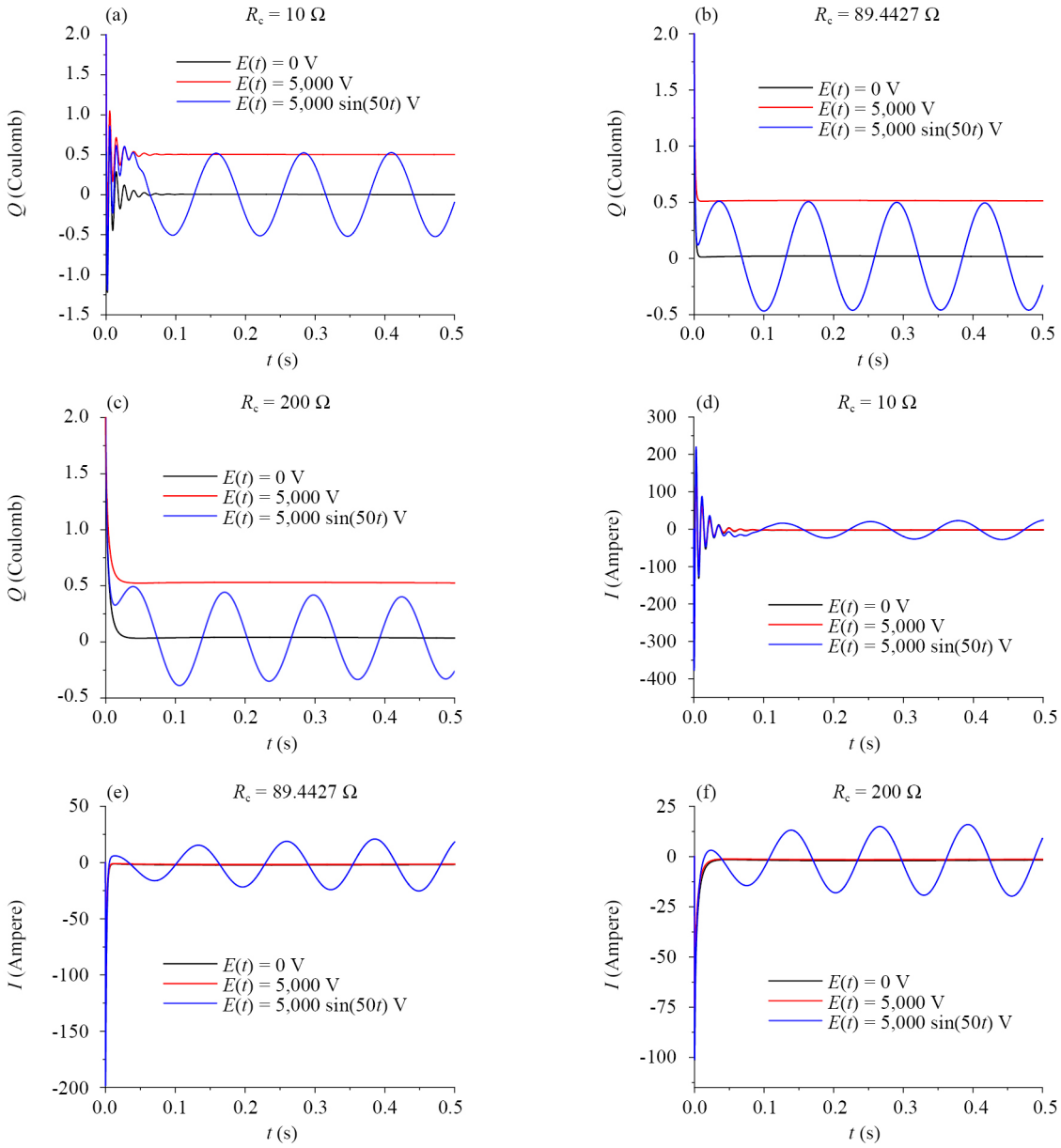


Figure 6. Time-domain current and charge responses of the fractional RLC circuit for a fractional order equal to $0.7 + 0.3t$, considering different resistance values and external excitations with five collocation points

For the integer-order case, $\alpha(t) = 1$, shown in Figures 4a–4f, the circuit exhibits the behavior expected for a classical RLC model, with negligible fractional-memory effects. The current and charge responses present a pronounced transient regime followed by distinct long-term behaviors depending on the external excitation. In the absence of external excitation, $E(t) = 0$, both the current and charge decay to zero, indicating the dissipation of the initially stored electrical energy. For the constant excitation, $E(t) = 5{,}000$ V, the current progressively approaches zero, whereas the charge converges to a nonzero steady-state value of approximately 0.5 C for the three resistance values considered. This behavior indicates that, in the steady state, the capacitor retains a finite amount of charge while the resistive branch no longer sustains a current. Under sinusoidal excitation, $E(t) = 5{,}000\sin(50t)$ V, both variables exhibit sustained oscillations after the initial transient. In particular, the charge oscillates around its equilibrium level with a finite amplitude, reflecting the continuous exchange of electrical energy between the capacitive and inductive elements induced by the periodic excitation. The amplitude and

transient characteristics of these oscillations are affected by the resistance, as the resistive element governs the dissipation of energy from the circuit. These observations are consistent with the dissipated-energy results reported in Table 3, which indicate a substantially larger energy dissipation for the integer-order formulation.

In contrast, the models defined by $\alpha(t) = 0.4 + 0.6/(1 + \exp(-4t))$ (Figures 5a–5f) and $\alpha(t) = 0.7 + 0.3t$ (Figures 5a–5f) exhibit a pronounced attenuation of the current response compared with the integer-order case. In both formulations, the fractional order remains substantially below unity over a significant portion of the simulation interval, thereby strengthening the memory effects of the system.

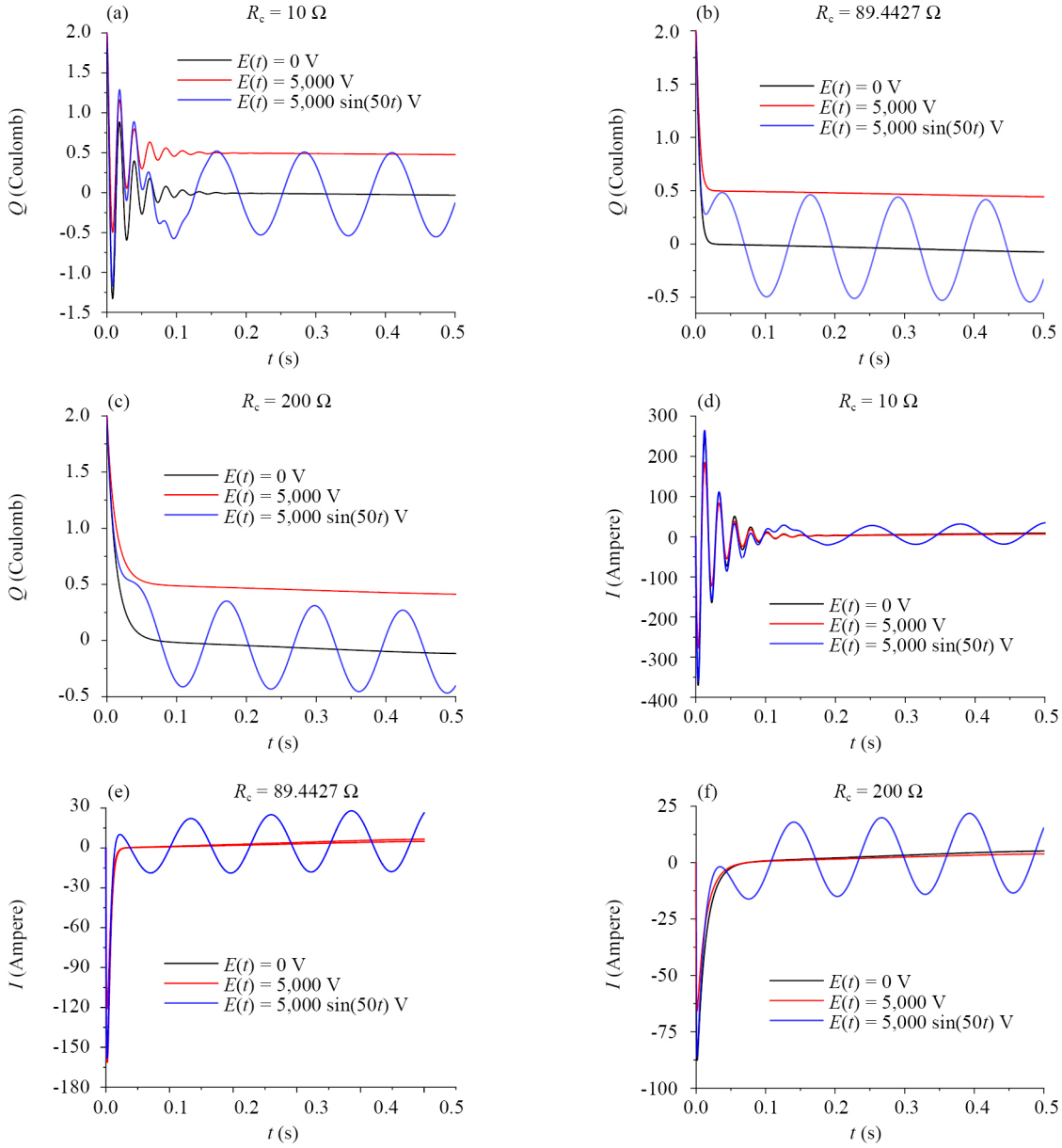


Figure 7. Time-domain current and charge responses of the fractional RLC circuit for a fractional order equal to $0.8 + 0.1\cos(4t)$, considering different resistance values and external excitations with five collocation points

This behavior results in smoother current profiles, reduced oscillation amplitudes, and lower current circulation, particularly during the transient regime. The corresponding charge responses also reveal the influence of fractional

memory. For $E(t) = 0$, the charge progressively decays toward zero, indicating that the initially stored electrical energy is gradually dissipated through the resistor. Under the constant excitation $E(t) = 5{,}000$ V, the charge approaches a nonzero steady-state value close to 0.5 C, while the current tends toward zero. Thus, despite the reduced current circulation, the capacitor retains a finite amount of stored charge in the steady state. Under sinusoidal excitation, the charge exhibits sustained oscillations, reflecting the continuous exchange of energy between the capacitor and inductor promoted by the periodic forcing. The reduced current amplitudes are accompanied by substantially lower resistive losses, with the dissipated energy decreasing by approximately 45–86% relative to the integer-order formulation, depending on the resistance and excitation conditions. These results indicate that fractional memory not only attenuates current circulation but also modifies the temporal distribution of energy storage within the reactive components.

The model associated with $\alpha(t) = 0.8 + 0.1\cos(4t)$ (Figures 7a–7f) exhibits an intermediate behavior between the nearly integer-order response and the responses associated with the lower fractional orders. Because the fractional order oscillates around 0.8, the memory effects remain significant throughout the simulation, although their intensity is lower than that observed for the formulations with smaller fractional orders. Accordingly, the current amplitudes are higher than those obtained with $\alpha(t) = 0.4 + 0.6/(1 + \exp(-4t))$ and $\alpha(t) = 0.7 + 0.3t$, but remain below those of the integer-order model. A similar intermediate behavior is observed in the charge responses. In the absence of external excitation, $Q(t)$ progressively approaches zero, whereas under constant excitation the charge converges to a finite value close to 0.5 C. For sinusoidal excitation, sustained charge oscillations are observed, indicating continuous energy exchange between the capacitive and inductive elements. Therefore, the oscillatory fractional-order function produces a response in which both current circulation and charge dynamics are intermediate between the lower-order fractional models and the integer-order formulation. This behavior is also consistent with the energy-based metrics in Table 3, which show higher dissipated-energy levels than those obtained for the two lower-order functions, while remaining below the values associated with $\alpha(t) = 1$.

For $E(t) = 0$, the responses shown in Figures 4–7 are purely transient and are governed by the energy initially stored in the capacitor and inductor. In this case, both $I(t)$ and $Q(t)$ progressively decay as the stored electrical energy is dissipated through the resistor. Under the constant excitation $E(t) = 5{,}000$ V, the current approaches zero while the charge converges to a finite steady-state value close to 0.5 C. This behavior is consistent with the classical capacitor (C) relation ($Q = CE$) at steady state and indicates that the continuous voltage excitation maintains a finite amount of electric charge in the capacitor even after the transient current has vanished. The fractional-order formulations modify the transient path toward this equilibrium state by introducing memory-dependent effects. In particular, lower fractional orders produce smoother current responses and lower resistive dissipation, while the charge remains capable of reaching a finite steady-state level. For the sinusoidal excitation, both current and charge exhibit sustained oscillations because energy is continuously supplied to the circuit. The charge oscillations provide an additional indication of the persistent exchange of energy between the capacitive and inductive elements, complementing the current-based analysis.

7. Conclusions

In this work, an extension of the Orthogonal Collocation Method (OCM) to variable-order fractional differential–algebraic systems was proposed and applied to the simulation of an RLC circuit. The formulation was specifically developed to accommodate fractional differential–algebraic equations with prescribed initial conditions and time-dependent fractional orders. Based on the numerical results obtained from the benchmark problems and the RLC circuit, the following conclusions can be drawn:

• The proposed methodology demonstrated excellent numerical accuracy for the mathematical benchmark problems, with errors substantially smaller than those reported in the literature and those obtained using the Adams Predictor–Corrector Method (APCM). The method also required lower computational times while employing only a small number of collocation points, achieving an attractive balance between accuracy and computational efficiency.

• For the mathematical problems investigated, the absolute error tends to increase near the end of the integration interval. This behavior is associated with the nature of initial-value problems and may be further influenced by the memory

effects inherent in fractional-order derivatives. Although this error accumulation did not compromise the accuracy of the present simulations, longer integration intervals may benefit from tighter convergence tolerances, refined collocation grids, or adaptive discretization strategies.

• The RLC simulations demonstrated that the fractional order can exert an influence on the circuit dynamics comparable to, or even greater than, that of the electrical resistance. When $\alpha(t) = 1$, the model recovers the classical integer-order behavior, characterized by stronger current circulation and higher resistive energy dissipation. As the fractional order decreases, memory effects become more pronounced, resulting in smoother current responses, reduced oscillation amplitudes, and lower dissipated energy.

• The inclusion of the capacitor charge response $Q(t)$ provides additional physical insight into the influence of fractional memory. In the absence of external excitation, both current and charge progressively decay toward zero as the initially stored electrical energy is dissipated. Under constant excitation, the current tends toward zero while the capacitor charge approaches approximately 0.5 C, corresponding to the expected steady-state value ($Q = CE$). Under sinusoidal excitation, both current and charge exhibit sustained oscillations, reflecting the continuous exchange of energy between the inductive and capacitive elements. Thus, the charge response complements the current-based analysis and provides a direct measure of the energy-storage behavior of the capacitor.

• The fractional-order formulations substantially reduce resistive energy dissipation compared with the integer-order model. The largest reductions occur for the lower fractional-order functions, for which the dissipated energy can decrease by approximately 86%. This reduction is directly associated with the attenuation of current circulation produced by the stronger memory effects.

• The formulation $\alpha(t) = 0.8 + 0.1\cos(4t)$ produces an intermediate dynamical regime. Its current amplitudes, charge oscillations, and dissipated-energy levels are generally higher than those obtained with the lower-order formulations $\alpha(t) = 0.4 + 0.6/(1 + \exp(-4t))$ and $\alpha(t) = 0.7 + 0.3t$, but remain below those of the integer-order model. This result highlights the possibility of continuously modulating the dynamic behavior of the circuit through the fractional-order function.

• The results also demonstrate that the effect of fractional memory cannot be evaluated solely from current amplitudes. The simultaneous analysis of $I(t)$ and $Q(t)$ reveals how changes in the fractional order affect both energy dissipation and energy storage. Consequently, the charge response may provide an additional observable for identifying or calibrating fractional-order models using experimental data.

• The flexibility introduced by fractional derivatives may enable closer agreement between mathematical models and experimental observations, potentially providing a more realistic representation of systems exhibiting memory and hereditary effects. Nevertheless, the fractional-order function should be selected within physically meaningful bounds, since unrestricted variations may produce responses that are inconsistent with the system under investigation.

• The proposed framework provides a flexible computational tool for investigating transient and steady-state responses of fractional-order electrical systems. Future work will focus on the experimental calibration and identification of the fractional-order function using measured current, voltage, and charge data, as well as on the extension of the methodology to inverse, reliability, and robustness analyses of fractional-order engineering systems.

As directions for future research, the proposed approach will be extended to reliability and robustness analyses of RLC circuits and other engineering systems. In addition, an inverse problem will be formulated and solved to estimate the fractional order directly from real experimental data.

Acknowledgments

Fran Sérgio Lobato gratefully acknowledges the Brazilian National Council for Scientific and Technological Development (CNPq) for the financial support provided through a research fellowship (Grant No. 309178/2023-1).

Finally, it is important to mention that a simplified version of this work was previously published in Portuguese in the proceedings of a scientific conference in 2025 [36]. The present manuscript substantially extends the conference paper by incorporating additional applications, more comprehensive analyses, and further numerical results. Although some of

the underlying methods and numerical data are shared between the two works, the current manuscript provides a broader investigation and additional contributions that go beyond the scope of the conference publication.

AI use disclosure

The authors declare that Artificial Intelligence (AI) tools were used during the revision of this manuscript. AI assistance was limited to improving the language, clarity, and readability of the manuscript. AI tools were not used to generate or modify research data, perform data analysis, interpret results, or formulate scientific conclusions. The authors remain fully responsible for the originality, accuracy, integrity, and ethical compliance of the manuscript.

Author contributions

William Júnio de Lima: Methodology, investigation, software, formal analysis, writing–review and editing and supervision. Fran Sérgio Lobato: Conceptualization, methodology, software, formal analysis, and writing–original draft. All authors reviewed and approved the final manuscript.

Funding

This research received no external funding.

Data availability

The computational code developed for this study is available from the corresponding author upon reasonable request.

Conflict of interest

The authors declare no conflict of interest.

References

[1] R. Almeida, D. Tavares, and D. F. M. Torres, *The Variable-Order Fractional Calculus of Variations*. Cham, Switzerland: Springer, 2019.

[2] V. E. Tarasov, *Fractional Dynamics: Applications of Fractional Calculus to Dynamics of Particles, Fields and Media*. Berlin, Heidelberg: Springer, 2010. Available: https://doi.org/10.1007/978-3-642-14003-7.

[3] H. Sun, A. Chang, Y. Zhang, and W. Chen, "A review on variable-order fractional differential equations: Mathematical foundations, physical models, numerical methods and applications," *Fractional Calculus and Applied Analysis*, vol. 22, no. 1, pp. 27-59, 2019.

[4] L. E. S. Ramirez and C. F. M. Coimbra, "A variable-order constitutive relation for viscoelasticity," *Annals of Physics*, vol. 519, no. 7-8, pp. 543-552, 2007.

[5] S. G. Samko and B. Ross, "Integration and differentiation to a variable fractional order," *Integral Transforms and Special Functions*, vol. 1, no. 4, pp. 277-300, 1993.

[6] C. M. Soon, C. F. M. Coimbra, and M. H. Kobayashi, "The variable viscoelasticity oscillator," *Annals of Physics*, vol. 517, no. 6, pp. 378-389, 2005. Available: https://doi.org/10.1002/andp.200410140.

[7] S. Patnaik and F. Semperlotti, "Variable-order particle dynamics: Formulation and application to the simulation of edge dislocations," *Philosophical Transactions of the Royal Society A*, vol. 378, no. 2172, p. 20190290, 2020.

[8] T. Błaszczyk, K. Bekus, K. Szajek, and W. Sumelka, "Approximation and application of the Riesz-Caputo fractional derivative of variable order with fixed memory," *Meccanica*, vol. 57, no. 4, pp. 861-870, 2021.

[9] M. Di Paola, G. Alotta, A. Burlon, and G. Failla, "A novel approach to nonlinear variable-order fractional viscoelasticity," *Philosophical Transactions of the Royal Society A*, vol. 378, no. 2172, p. 20190296, 2020.

[10] S. Patnaik, M. Jokar, and F. Semperlotti, "Variable-order approach to nonlocal elasticity: Theoretical formulation, order identification via deep learning, and applications," *Computational Mechanics*, vol. 69, no. 1, pp. 267-298, 2022.

[11] S. Shen, F. Liu, J. Chen, I. Turner, and V. Anh, "Numerical techniques for the variable-order time fractional diffusion equation," *Applied Mathematics and Computation*, vol. 218, no. 22, pp. 10861-10870, 2012.

[12] C. M. Chen, F. Liu, V. Anh, and I. Turner, "Numerical schemes with high spatial accuracy for a variable-order anomalous subdiffusion equation," *SIAM Journal on Scientific Computing*, vol. 32, no. 4, pp. 1740-1760, 2010.

[13] J. X. Cao and Y. N. Qiu, "A high-order numerical scheme for variable-order fractional ordinary differential equations," *Applied Mathematics Letters*, vol. 61, pp. 88-94, 2016.

[14] M. Zayernouri and G. E. Karniadakis, "Fractional spectral collocation methods for linear and nonlinear variable-order fractional partial differential equations," *Journal of Computational Physics*, vol. 293, pp. 312-338, 2015.

[15] X. Zhao, Z. Z. Sun, and G. E. Karniadakis, "Second-order approximations for variable-order fractional derivatives: Algorithms and applications," *Journal of Computational Physics*, vol. 293, pp. 184-200, 2015.

[16] X. Li, H. Li, and B. Wu, "A new numerical method for variable-order fractional functional differential equations," *Applied Mathematics Letters*, vol. 68, pp. 80-86, 2017.

[17] X. Y. Li and B. Y. Wu, "A numerical technique for variable fractional functional boundary value problems," *Applied Mathematics Letters*, vol. 43, pp. 108-113, 2015.

[18] S. Nemati, P. M. Lima, and D. F. M. Torres, "Numerical solution of variable-order fractional differential equations using Bernoulli polynomials," *Fractal and Fractional*, vol. 5, no. 4, p. 219, 2021.

[19] N. Ayazi, P. Mokhtary, and B. P. Moghaddam, "Efficiently solving fractional delay differential equations of variable order via an adjusted spectral element approach," *Chaos, Solitons & Fractals*, vol. 181, p. 114635, 2024. Available: https://doi.org/10.1016/j.chaos.2024.114635.

[20] M. H. Derakhshan, "A numerical technique for solving variable order time fractional differential-integro equations," *Communications in Mathematics*, vol. 32, no. 1, pp. 129-147, 2024. Available: https://doi.org/10.46298/cm.10822.

[21] H. M. Ahmed, M. Izadi, and C. Cattani, "A spectral approach to variable-order fractional differential equations: Improved operational matrices for fractional Jacobi functions," *Mathematics*, vol. 13, no. 16, p. 2544, 2025. Available: https://doi.org/10.3390/math13162544.

[22] O. Postavaru and A. Toma, "A fractional hybrid function composed of block-pulses and fractional Fibonacci polynomials for solving multiterm fractional variable-order differential equations," *Computational and Applied Mathematics*, vol. 44, p. 151, 2025. Available: https://doi.org/10.1007/s40314-025-03110-4.

[23] M. S. Al-Sharif, A. I. Ahmed, and M. S. Salim, "Fractional-order Chelyshkov collocation method for solving variable-order fractional differential equations," *Journal of Inequalities and Applications*, vol. 2026, no. 1, p. 9, 2026. Available: https://doi.org/10.1186/s13660-025-03409-0.

[24] J. F. Gómez-Aguilar, A. Atangana, and V. F. Morales-Delgado, "Electrical circuits RC, LC, and RL described by Atangana-Baleanu fractional derivatives," *International Journal of Circuit Theory and Applications*, vol. 45, no. 11, pp. 1514-1533, 2017. Available: https://doi.org/10.1002/cta.2348.

[25] N. Sene and J. F. Gómez-Aguilar, "Analytical solutions of electrical circuits considering certain generalized fractional derivatives," *The European Physical Journal Plus*, vol. 134, no. 6, p. 260, 2019. Available: https://doi.org/10.1140/epjp/i2019-12618-x.

[26] S. Naveen, V. Parthiban, and M. I. Abbas, "Qualitative analysis of RLC circuit described by Hilfer derivative with numerical treatment using the Lagrange polynomial method," *Fractal and Fractional*, vol. 7, no. 11, p. 804, 2023. Available: https://doi.org/10.3390/fractalfract7110804.

[27] M. Malarvizhi, S. Karunanithi, and N. Gajalakshmi, "Numerical analysis using RK-4 in transient analysis of RLC circuit," *Advances in Mathematics: Scientific Journal*, vol. 9, no. 8, pp. 6115-6124, 2020.

[28] S. Naveen and V. Parthiban, "Variable-order Caputo derivative of LC and RC circuits system with numerical analysis," *International Journal of Circuit Theory and Applications*, vol. 53, no. 5, pp. 3136-3156, 2025. Available: https://doi.org/10.1002/cta.4240.

[29] C. K. Alexander and M. N. O. Sadiku, *Fundamentals of Electric Circuits*, 6th ed., New York, NY, USA: McGraw-Hill Education, 2017.

[30] I. Podlubny, *Fractional Differential Equations*, Mathematics in Science and Engineering, vol. 198. San Diego, CA, USA: Academic Press, 1999.

[31] S. Naveen and V. Parthiban, "Application of Newton's polynomial interpolation scheme for variable order fractional derivative with power-law kernel," *Scientific Reports*, vol. 14, p. 16090, 2024. Available: https://doi.org/10.1038/s41598-024-66494-z.

[32] C. Canuto, M. Y. Hussaini, A. Quarteroni, and T. A. Zang, *Spectral Methods: Fundamentals in Single Domains*. Berlin, Germany: Springer, 2006.

[33] M. Mortezaee, M. Ghovatmand, and A. Nazemi, "Solving variable-order fractional differential algebraic equations via generalized fuzzy hyperbolic model with application in electric circuit modeling," *Soft Computing*, vol. 24, no. 22, pp. 16745-16758, 2020. Available: https://doi.org/10.1007/s00500-020-04969-7.

[34] D. Sun, S. Tian, X. Jiao, and Y. Jiang, "Discussions for the charging efficiency of the resistor-capacitor and resistor-inductor-capacitor series circuits under different excitation sources," *Energy Reports*, vol. 8, pp. 300-306, 2022. Available: https://doi.org/10.1016/j.egyr.2022.09.163.

[35] S. Paul, A. M. Schlaffer, and J. Nossek, "Optimal charging of capacitors," *IEEE Transactions on Circuits and Systems I: Fundamental Theory and Applications*, vol. 47, no. 7, pp. 1009-1016, 2000. Available: https://doi.org/10.1109/81.855456.

[36] W. J. Lima, S. E. S. Faria, and F. L. Lobato, "Analysis of an RLC circuit with fractional derivative of variable order using the Orthogonal Collocation Method," (in Portuguese), in Proceedings of the National Meeting on Computational Modeling and Meeting on Materials Science and Technology, 2025. [Online]. Available: https://www.even3.com.br/anais/enmc-2025/1249323-ana%3flise-de-um-circuito-rlc-com-derivada-fraciona%3fria-com-ordem-varia%3fvel-usando-o-me%3ftodo-da-colocac%3fa~o-ortogo. [Accessed Oct. 21, 2026].